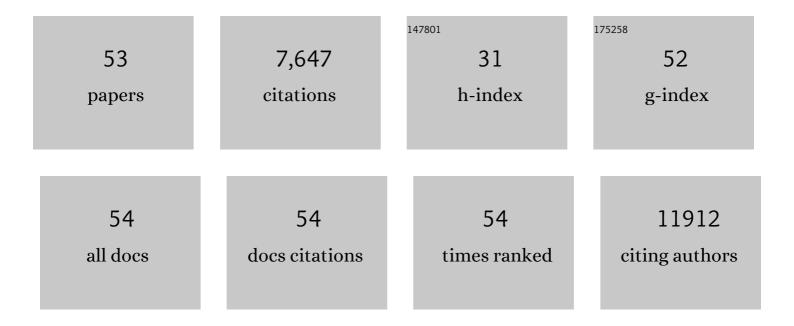
Scott Cushing

List of Publications by Year in descending order

Source: https://exaly.com/author-pdf/8874668/publications.pdf Version: 2024-02-01



#	Article	IF	CITATIONS
1	Single-Photon Scattering Can Account for the Discrepancies among Entangled Two-Photon Measurement Techniques. Journal of Physical Chemistry Letters, 2022, 13, 4934-4940.	4.6	12
2	<i>Ab Initio</i> Prediction of Excited-State and Polaron Effects in Transient XUV Measurements of α-Fe ₂ O ₃ . Journal of the American Chemical Society, 2022, 144, 12834-12841.	13.7	10
3	Electron thermalization and relaxation in laser-heated nickel by few-femtosecond core-level transient absorption spectroscopy. Physical Review B, 2021, 103, .	3.2	21
4	Characterization of Carrier Cooling Bottleneck in Silicon Nanoparticles by Extreme Ultraviolet (XUV) Transient Absorption Spectroscopy. Journal of Physical Chemistry C, 2021, 125, 9319-9329.	3.1	6
5	Designing high-power, octave spanning entangled photon sources for quantum spectroscopy. Journal of Chemical Physics, 2021, 154, 244201.	3.0	7
6	Element-specific electronic and structural dynamics using transient XUV and soft X-ray spectroscopy. CheM, 2021, 7, 2569-2584.	11.7	14
7	Molecular hot spots in surface-enhanced Raman scattering. Nanoscale, 2020, 12, 22036-22041.	5.6	33
8	Layer-resolved ultrafast extreme ultraviolet measurement of hole transport in a Ni-TiO ₂ -Si photoanode. Science Advances, 2020, 6, eaay6650.	10.3	29
9	Entangled light–matter interactions and spectroscopy. Journal of Materials Chemistry C, 2020, 8, 10732-10741.	5.5	34
10	Transient Extreme Ultraviolet Measurement of Carrier Dynamics in Solar Fuel Materials. , 2020, , .		0
11	Differentiating Photoexcited Carrier and Phonon Dynamics in the Δ, <i>L</i> , and Γ Valleys of Si(100) with Transient Extreme Ultraviolet Spectroscopy. Journal of Physical Chemistry C, 2019, 123, 3343-3352.	3.1	23
12	Transient extreme ultraviolet measurement of element-specific charge transfer dynamics in multiple-material junctions. , 2019, , .		0
13	Hot phonon and carrier relaxation in Si(100) determined by transient extreme ultraviolet spectroscopy. Structural Dynamics, 2018, 5, 054302.	2.3	39
14	The ultrafast X-ray spectroscopic revolution in chemical dynamics. Nature Reviews Chemistry, 2018, 2, 82-94.	30.2	215
15	Femtosecond tracking of carrier relaxation in germanium with extreme ultraviolet transient reflectivity. Physical Review B, 2018, 97, .	3.2	40
16	Photoexcited Small Polaron Formation in Goethite (α-FeOOH) Nanorods Probed by Transient Extreme Ultraviolet Spectroscopy. Journal of Physical Chemistry Letters, 2018, 9, 4120-4124.	4.6	26
17	Effects of Defects on Photocatalytic Activity of Hydrogen-Treated Titanium Oxide Nanobelts. ACS Catalysis, 2017, 7, 1742-1748.	11.2	173
18	Excitation wavelength dependent fluorescence of graphene oxide controlled by strain. Nanoscale, 2017, 9, 2240-2245.	5.6	21

SCOTT CUSHING

#	Article	IF	CITATIONS
19	Direct and simultaneous observation of ultrafast electron and hole dynamics in germanium. Nature Communications, 2017, 8, 15734.	12.8	117
20	Ultrafast carrier thermalization and trapping in silicon-germanium alloy probed by extreme ultraviolet transient absorption spectroscopy. Structural Dynamics, 2017, 4, 044029.	2.3	42
21	Measuring the Surface Photovoltage of a Schottky Barrier under Intense Light Conditions: Zn/p-Si(100) by Laser Time-Resolved Extreme Ultraviolet Photoelectron Spectroscopy. Journal of Physical Chemistry C, 2017, 121, 21904-21912.	3.1	9
22	Plasmonic hot carriers skip out in femtoseconds. Nature Photonics, 2017, 11, 748-749.	31.4	21
23	Excitation-wavelength-dependent small polaron trapping of photoexcited carriers in α-Fe2O3. Nature Materials, 2017, 16, 819-825.	27.5	178
24	Investigation of the plasmonic effect in air-processed PbS/CdS core–shell quantum dot based solar cells. Journal of Materials Chemistry A, 2016, 4, 13071-13080.	10.3	18
25	Distinguishing surface effects of gold nanoparticles from plasmonic effect on photoelectrochemical water splitting by hematite. Journal of Materials Research, 2016, 31, 1608-1615.	2.6	25
26	Progress and Perspectives of Plasmon-Enhanced Solar Energy Conversion. Journal of Physical Chemistry Letters, 2016, 7, 666-675.	4.6	220
27	A Surface-Enhanced Raman Scattering Sensor Integrated with Battery-Controlled Fluidic Device for Capture and Detection of Trace Small Molecules. Scientific Reports, 2015, 5, 12865.	3.3	19
28	A gold nanohole array based surface-enhanced Raman scattering biosensor for detection of silver(<scp>i</scp>) and mercury(<scp>ii</scp>) in human saliva. Nanoscale, 2015, 7, 11005-11012.	5.6	98
29	Enhancement of Solar Hydrogen Generation by Synergistic Interaction of La ₂ Ti ₂ O ₇ Photocatalyst with Plasmonic Gold Nanoparticles and Reduced Graphene Oxide Nanosheets. ACS Catalysis, 2015, 5, 1949-1955.	11.2	122
30	Tailoring plasmonic properties of gold nanohole arrays for surface-enhanced Raman scattering. Physical Chemistry Chemical Physics, 2015, 17, 21211-21219.	2.8	69
31	Inverting Transient Absorption Data to Determine Transfer Rates in Quantum Dot–TiO ₂ Heterostructures. Journal of Physical Chemistry C, 2015, 119, 6337-6343.	3.1	24
32	Controlling Plasmon-Induced Resonance Energy Transfer and Hot Electron Injection Processes in Metal@TiO ₂ Core–Shell Nanoparticles. Journal of Physical Chemistry C, 2015, 119, 16239-16244.	3.1	219
33	Band gap narrowing in nitrogen-doped La ₂ Ti ₂ O ₇ predicted by density-functional theory calculations. Physical Chemistry Chemical Physics, 2015, 17, 8994-9000.	2.8	37
34	Theoretical maximum efficiency of solar energy conversion in plasmonic metal–semiconductor heterojunctions. Physical Chemistry Chemical Physics, 2015, 17, 30013-30022.	2.8	58
35	Investigation of band gap narrowing in nitrogen-doped La ₂ Ti ₂ O ₇ with transient absorption spectroscopy. Physical Chemistry Chemical Physics, 2015, 17, 31039-31043.	2.8	15
36	Plasmon-induced resonance energy transfer for solar energy conversion. Nature Photonics, 2015, 9, 601-607.	31.4	587

SCOTT CUSHING

#	Article	IF	CITATIONS
37	Plasmon-enhanced optical sensors: a review. Analyst, The, 2015, 140, 386-406.	3.5	784
38	Photoluminescence spectroscopy of YVO4:Eu3+ nanoparticles with aromatic linker molecules: A precursor to biomedical functionalization. Journal of Applied Physics, 2014, 115, 163107.	2.5	13
39	Origin of Strong Excitation Wavelength Dependent Fluorescence of Graphene Oxide. ACS Nano, 2014, 8, 1002-1013.	14.6	328
40	Solar Hydrogen Generation by a CdS-Au-TiO ₂ Sandwich Nanorod Array Enhanced with Au Nanoparticle as Electron Relay and Plasmonic Photosensitizer. Journal of the American Chemical Society, 2014, 136, 8438-8449.	13.7	533
41	Photocatalytic hydrogen generation enhanced by band gap narrowing and improved charge carrier mobility in AgTaO3 by compensated co-doping. Physical Chemistry Chemical Physics, 2013, 15, 16220.	2.8	54
42	Plasmonic Nanorice Antenna on Triangle Nanoarray for Surface-Enhanced Raman Scattering Detection of Hepatitis B Virus DNA. Analytical Chemistry, 2013, 85, 2072-2078.	6.5	141
43	Ag@Cu ₂ 0 Core-Shell Nanoparticles as Visible-Light Plasmonic Photocatalysts. ACS Catalysis, 2013, 3, 47-51.	11.2	471
44	Photocatalytic Water Oxidation by Hematite/Reduced Graphene Oxide Composites. ACS Catalysis, 2013, 3, 746-751.	11.2	226
45	Asymmetric Silver "Nanocarrot―Structures: Solution Synthesis and Their Asymmetric Plasmonic Resonances. Journal of the American Chemical Society, 2013, 135, 9616-9619.	13.7	43
46	Three-Dimensional Hierarchical Plasmonic Nano-Architecture Enhanced Surface-Enhanced Raman Scattering Immunosensor for Cancer Biomarker Detection in Blood Plasma. ACS Nano, 2013, 7, 4967-4976.	14.6	241
47	Solar Hydrogen Generation by Nanoscale <i>p–n</i> Junction of <i>p</i> -type Molybdenum Disulfide/ <i>n</i> -type Nitrogen-Doped Reduced Graphene Oxide. Journal of the American Chemical Society, 2013, 135, 10286-10289.	13.7	599
48	Photocatalytic Activity Enhanced by Plasmonic Resonant Energy Transfer from Metal to Semiconductor. Journal of the American Chemical Society, 2012, 134, 15033-15041.	13.7	1,052
49	Fingerprinting photoluminescence of functional groups in graphene oxide. Journal of Materials Chemistry, 2012, 22, 23374.	6.7	198
50	Shape-dependent surface-enhanced Raman scattering in gold–Raman-probe–silica sandwiched nanoparticles for biocompatible applications. Nanotechnology, 2012, 23, 115501.	2.6	166
51	Size-Dependent Energy Transfer between CdSe/ZnS Quantum Dots and Gold Nanoparticles. Journal of Physical Chemistry Letters, 2011, 2, 2125-2129.	4.6	200
52	Origin of localized surface plasmon resonances in thin silver film over nanosphere patterns. Applied Physics A: Materials Science and Processing, 2011, 103, 955-958.	2.3	14
53	Electrodeposition of Poly(phenylene oxide) Nanoscale Patterns with Nanosphere Lithography. ECS Transactions, 2009, 19, 159-164.	0.5	2